

Photophysical characterization and photodynamic activity of metallo 5-(4-(trimethylammonium)phenyl)-10,15,20-tris(2,4,6-trimethoxyphenyl)porphyrin in homogeneous and biomimetic media

M. Elisa Milanesio, M. Gabriela Alvarez, Sonia G. Bertolotti and Edgardo N. Durantini*

Received 20th March 2008, Accepted 11th June 2008

First published as an Advance Article on the web 28th June 2008

DOI: 10.1039/b804848g

The photophysical properties and photodynamic effect of Zn(II), Pd(II), Cu(II) and free-base 5-(4-(trimethylammonium)phenyl)-10,15,20-tris(2,4,6-trimethoxy phenyl)porphyrin (H₂P) iodide have been studied in *N,N*-dimethylformamide (DMF) and in different biomimetic systems. The absorption, fluorescence, triplet state and singlet molecular oxygen production of the metal complexes were all referred to H₂P. The photodynamic activity was first analyzed using 9,10-dimethylanthracene and guanosine 5'-monophosphate in *N,N*-dimethylformamide. The photooxidation processes were also investigated in benzene/benzyl-*n*-hexadecyldimethyl ammonium chloride/water reverse micelles. Photosensitization efficiency of these porphyrins was H₂P ~ ZnP > PdP in homogeneous solution and ZnP > H₂P > PdP in micelles, whereas no photooxidation effect was detected using the Cu(II) complex. Human erythrocytes were used as a biological membrane model. The photohemolytic activity depended on irradiation time, sensitizer and concentration of the agent. When cells were treated with 1 μM sensitizer, the hemolytic activity was H₂P > ZnP >> CuP. However, it was H₂P > ZnP ~ CuP using 5 μM of the respective porphyrin. Although CuP could undergo a type I photoreaction, in all cases the photohemolytic effect considerably diminishes in anoxic conditions, indicating that an oxygen atmosphere is required for the mechanism of cellular membrane damage. The behavior of these amphiphilic metallo porphyrins provides information on the photodynamic activity of these agents in biomimetic microenvironments.

Introduction

Porphyrin derivatives have shown great potential as phototherapeutic agents for the treatment of a variety of oncological and non-oncological diseases.¹⁻⁴ Photodynamic therapy (PDT) of cancer involves the administration of a photosensitizer, which is selectively incorporated in tumor cells. The subsequent exposure to visible light in the presence of oxygen specifically inactivates the neoplastic tissue.¹ Two oxidative mechanisms are considered to be principally implicated in the photodamage of cells. In the type I photochemical reaction, the photosensitizer interacts with a biomolecule to produce free radicals, while in the type II mechanism, singlet molecular oxygen, O₂(¹Δ_g), is produced as the main species responsible for cellular inactivation.⁵ Depending on the experimental conditions, these mechanisms can occur simultaneously and the ratio between the two processes is influenced by the sensitizer, substrate and the nature of the medium.⁶

In the last years several new sensitizers have been proposed with improved physical, chemical and therapeutic properties for PDT.⁷ Various classes of photosensitizers are presently in clinical use or in stages of development in biological media.⁸ Adequate photosensitizers are deemed to have specific chemical and biological properties.¹ Two of the photochemical requisites are a high absorption coefficient in the visible region of the spectrum

and a long lifetime of triplet excited state to produce efficiently O₂(¹Δ_g).

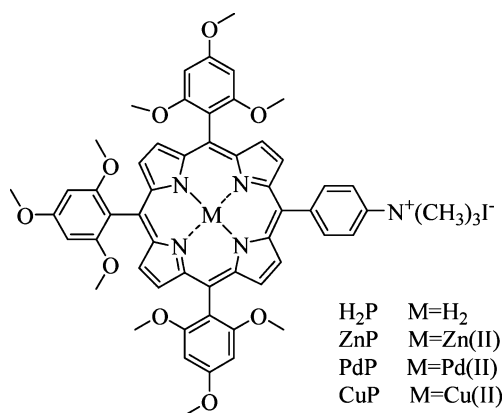
The photophysical properties of free-base porphyrins are significantly modified by the nature of the central metal ion.⁹⁻¹⁴ The characteristics of metalloporphyrins containing regular metals ions, such as Zn, with d⁰ or d¹⁰ configuration are determined essentially by the π electrons of the macrocycle ring. On the other hand, in metalloporphyrin forming complexes with a transition metal with incomplete d orbitals, for example Cu, these orbitals can significantly integrate with the orbitals of the porphyrin ring. Thus, the excited state of these complexes have short lifetime and the quantum yield of triplet state formation is very low.

Solubilization of photosensitizers plays an important role in biological processes. Water-soluble and water-insoluble compounds can be dissolved simultaneously in reverse micelles. In these microheterogeneous systems, a solute can be located in a variety of microenvironments, namely the organic surrounded solvent, the water pool or at the micellar interface.¹⁵ Therefore, reverse micelles are frequently used as an interesting model to mimic the water pockets often found in various bioaggregates such as proteins, enzymes and membranes.^{13,16-18} Biological membranes seem to be important targets for many antineoplastic photosensitizer agents. In this sense, mammalian erythrocytes constitute an attractive and suitable model system to study membrane photomodification.¹⁹⁻²⁴ Recent investigations show that red blood cells are useful to elucidate the cellular and molecular principles of PDT. Photodynamic damage of erythrocyte membranes starts with potassium release. Hemolysis just indicates disruption of the cell membranes. In

Departamento de Química, Universidad Nacional de Río Cuarto, Río Cuarto, Agencia Postal Nro. 3, X5804BYA, Río Cuarto, Argentina. E-mail: edurantini@exa.unrc.edu.ar

accordance with cell-culture assays where cell death is monitored by membrane disruption, hemolysis of red blood cells can be regarded as a mode of measuring death of erythrocytes.²⁵

In previous studies, the photodynamic activity of the free-base 5,10,15,20-tetrakis(4-methoxyphenyl)porphyrin (TMP) was compared with that produced by its metal complexes, both in reverse micelle of *n*-heptane/sodium bis(2-ethylhexyl)sulfosuccinate (AOT)/water and on Hep-2 human larynx-carcinoma cell line. Production of O₂(¹Δ_g) was increased by complexation with Zn(II) and Cd(II), which was associated with a higher phototoxicity.¹³ Similar behavior was also found for 5-(4-carboxyphenyl)-10,15,20-tris(4-methylphenyl) porphyrin forming complexes with Zn(II) and Pd(II).¹⁶ In addition, *in vitro* investigations showed that 5-(4-(trimethylammonium)phenyl)-10,15,20-tris(2,4,6-trimethoxyphenyl)porphyrin iodide (H₂P) is an efficient agent with interesting PDT application.^{26,27} The amphiphilic character of H₂P produces a better accumulation in subcellular compartments, which is a prerequisite for an effective photosensitization. Pharmacokinetic and phototherapeutic studies *in vivo* using Balb/c mouse cancer model indicated that H₂P is preferentially accumulated in tumor with respect to skin and muscle and PDT treatment with this agent resulted in a complete tumor regression.²⁸ Therefore, in this work we expanded the knowledge relative to metal derivatives of H₂P with Zn(II), Pd(II) and Cu(II) (Scheme 1). The photophysical and photodynamic characteristics of these photosensitizers were studied in homogeneous medium and reverse micelles biomimetic system. Photodynamic action was then performed *in vitro* using erythrocyte cells under different conditions to obtain information about the effect produced by metal complexation of this asymmetrically substituted cationic porphyrin.



Scheme 1 Molecular structures of the studied porphyrins.

Materials and methods

General

UV-visible absorption and fluorescence spectra were recorded on a Shimadzu UV-2401 PC spectrometer and on a Spex FluoroMax fluorometer, respectively. FAB mass spectra were taken with a ZAB-SEQ Micromass equipment. All the chemicals from Aldrich (Milwaukee, WI, USA) were used without further purification. Guanosine 5'-monophosphate (GMP) from Sigma (St. Louis, MO, USA) was used as received. Benzyl-*n*-hexadecyldimethylammonium

chloride (BHDC) from Sigma was recrystallized twice from ethyl acetate and dry under vacuum over P₂O₅. Solvents (GR grade) from Merck (Darmstadt, Germany) were distilled. Ultrapure water was obtained from a Labconco (Kansas, MO, USA) equipment model 90901-01.

Sensitizers

5-(4-(Trimethylammonium)phenyl)-10,15,20-tris(2,4,6-trimethoxyphenyl)porphyrin iodide (H₂P) was synthesized as previously described.²⁶

Preparation of zinc (II) 5-(4-(trimethylammonium)phenyl)-10,15,20-tris(2,4,6-trimethoxyphenyl)porphyrin iodide (ZnP). A solution of H₂P (20 mg, 0.019 mmol) in 7 ml of dichloromethane was treated with 3 mL of a saturated solution of zinc(II) acetate in methanol. The mixture was stirred for 30 min in argon atmosphere at room temperature. After that, the solution was treated with water (30 mL) and the organic phase was extracted with three portions of chloroform (20 mL each). The solvents were evaporated under reduced pressure. The reaction afforded 18 mg (85%) of pure ZnP. MS [*m/z*] 1004 (M⁺ – I) (1004.3213 calculated for C₅₆H₅₄N₅O₉Zn).

Preparation of palladium (II) 5-(4-(trimethylammonium)phenyl)-10,15,20-tris(2,4,6-trimethoxyphenyl) porphyrin iodide (PdP). To a solution of H₂P (20 mg, 0.019 mmol) in 10 mL of *N,N*-dimethylformamide (DMF) palladium (II) chloride (50 mg, 0.28 mmol) was added. The mixture was stirred for 4 h at reflux in atmosphere of argon. The product was extracted as described above for ZnP yielding 28 mg (83%) of PdP. MS *m/z* 1046 (M⁺ – I) (1046.2956 calculated for C₅₆H₅₄N₅O₉Pd).

Preparation of copper (II) 5-(4-(trimethylammonium)phenyl)-10,15,20-tris(2,4,6-trimethoxyphenyl) porphyrin iodide (CuP). A solution of H₂P (20 mg, 0.019 mmol), copper(II) acetate monohydrate (110 mg, 0.55 mmol) and glacial acetic acid (5 mL) in 3 mL of chloroform was refluxed for 2 h in argon atmosphere. The product was extracted as described above for ZnP yielding 16 mg (75%) of pure CuP. MS [*m/z*] 1003 (M⁺ – I) (1003.3218 calculated for C₅₆H₅₄N₅O₉Cu).

Spectroscopic and photophysical studies

Absorption and fluorescence spectra were recorded at 25.0 ± 0.5 °C using 1 cm path length quartz cells. The fluorescence quantum yield (Φ_F) of porphyrins were calculated by comparison of the area below the corrected emission spectrum in DMF with that of tetraphenylporphyrin (TPP) as a reference (Φ_F = 0.12).²⁶ The emission spectra were recorded exciting the samples at λ_{exc} = 550 nm. The energy of the singlet-state was deduced from the intersection of the normalized absorption and fluorescence curves. Fluorescence lifetimes (τ_s) of porphyrins were determined by the time-correlated singlet photon counting technique (Edinburgh Instrument OB900).

Sensitization of O₂(¹Δ_g) was measured by using the time-resolved phosphorescence detection method (TRPD). A Q-switched Nd:YAG laser (Spectron) was used as the excitation source operating at 532 nm (20 ns halfwidth) in order to excite the porphyrins. The emitted radiation (mainly 1270 nm) was detected at right angles with an amplified Judson J16/8Sp germanium

detector, after passing through appropriate filters. The output of the detector was coupled to a digital oscilloscope (Hewlett-Packard HP-54504 A). About twenty shots were usually needed for averaging decay times, in order to get a good signal to noise ratio. No change in the porphyrin absorption spectrum was observed after these experiments, indicating no significant photodegradation of the sensitizer. The averaged signals were analyzed as single exponential decays. The absorbance of the sample and reference were matched at the irradiation wavelength. Measurements of these solutions under the same conditions afforded Φ_{Δ} for the studied porphyrins by direct comparison of the slopes, in the linear region, of the plots of the amplitude of phosphorescence extrapolated to zero time vs. the laser-total energy.²⁹ TPP in DMF was used as a reference ($\Phi_{\Delta} = 0.62$).²⁶ The bimolecular constants of triplet excited state quenching of the photosensitizers by oxygen were calculated from known oxygen concentrations³⁰ and the measured rate constants of deactivation of the triplet states for solutions saturated with oxygen, air and argon. The triplet-triplet absorption spectra of sensitizers were determined in deoxygenated DMF solutions. Transient absorption measurements were made using laser flash photolysis equipment previously described.³¹

Steady state photolysis

Solutions of 9,10-dimethylanthracene (DMA, 35 μM) and photosensitizer (Soret band, absorbance 0.1) in DMF (2 mL) in quartz cuvettes were irradiated with monochromatic light at the Soret band with light from a 75 W high-pressure Xe lamp through a high intensity grating monochromator (Photon Technology Instrument). The fluence rate was determined as 2.3 mW cm^{-2} (Radiometer Laser Mate-Q, Coherent). The kinetics of DMA photooxidation were studied by following the decrease of the absorbance (A) at $\lambda_{\text{max}} = 378 \text{ nm}$. The observed rate constants (k_{obs}) were obtained by a linear least-squares fit of the semilogarithmic plot of $\ln A_0/A$ vs. time. Photooxidation of DMA was also used as indirect method to determine $\text{O}_2(^1\Delta_{\text{g}})$ production by the photosensitizers.³² Measurements of the sample and reference under the same conditions afforded Φ_{Δ} for porphyrins by direct comparison of the slopes in the linear region of the plots. The studies in the presence of GMP (100 μM) were performed irradiating the samples at Soret band with a fluence rate of 6.1 mW cm^{-2} . All the experiment were performed at $25.0 \pm 0.5 \text{ }^{\circ}\text{C}$. The pooled standard deviation of the kinetic data, using different prepared samples, was less than 10%.

Studies in reverse micelles

Studies in reverse micelles were performed using a stock solution of benzyl-*n*-hexadecyldimethyl ammonium chloride (BHDC) 0.1 M, which was prepared by weighing and dilution in benzene. The addition of water to the corresponding solution was performed using a calibrated microsyringe. The amount of water present in the system was expressed as the molar ratio between water and the BHDC present in the reverse micelle ($W_0 = [\text{H}_2\text{O}]/[\text{BHDC}]$). In all experiments, $W_0 = 10$ was used. The mixtures were sonicated for about 10 s to obtain perfectly clear micellar system.¹³

The binding constants, $K_{\text{b}} = [\text{porphyrin}_{\text{b}}]/[\text{porphyrin}_{\text{f}}][\text{BHDC}]$ (where the terms $[\text{porphyrin}_{\text{b}}]$ and $[\text{porphyrin}_{\text{f}}]$ refer to the

concentration of bound and free porphyrin, respectively, and $[\text{BHDC}]$ is the total surfactant concentration) were calculated by using the Ketelaar's equation from the spectral changes at the Soret band upon varying the BHDC concentration.¹⁶

$$\frac{1}{A - A_{\text{Bz}}} = \frac{1}{(\varepsilon_{\text{b}} - \varepsilon_{\text{Bz}})[\text{porphyrin}]_0} + \frac{1}{(\varepsilon_{\text{b}} - \varepsilon_{\text{Bz}})[\text{porphyrin}]_0 K_{\text{b}}[\text{BHDC}]} \quad (1)$$

where $[\text{porphyrin}]_0$ is the initial concentration of the porphyrin, A is the absorbance at different $[\text{BHDC}]$, A_{Bz} is the absorbance in benzene, ε_{b} and ε_{Bz} are the molar absorptivity for the porphyrin bound to the interface and in the organic medium, respectively. Plotting the left-hand side term of eqn (1) vs. $1/[\text{BHDC}]$, the value of K_{b} is obtained from the intercept to slope ratio.¹⁶

Partition coefficient measurements

1-Octanol/water partition coefficients (P) were determined at $25 \text{ }^{\circ}\text{C}$ using equal volumes of water (2 mL) and 1-octanol (2 mL). Typically, a solution of each porphyrin ($\sim 10 \mu\text{M}$) was stirred in the thermostat after the equilibrium was reached (8 h). An aliquot (100 μL) of aqueous and organic phases were dissolved in 2 mL of DMF and the final porphyrin concentration determined by absorption spectroscopy.¹⁶

Studies in human erythrocytes

Human erythrocytes were obtained from healthy donors. After extraction, the whole blood was taken into anticoagulant EDTA, centrifuged (3000 rev min^{-1}) to remove plasma and the leukocyte layer, washed three times with phosphate buffer saline (PBS) solution (137 mM NaCl, 2.7 mM KCl, 1.5 mM KH_2PO_4 and 8 mM Na_2HPO_4) and centrifuged again. Erythrocytes were re-suspended in saline solution (0.9% NaCl) to get a concentration of $\sim 10^9$ red blood cells mL^{-1} and maintained at $4 \text{ }^{\circ}\text{C}$ until use.^{19,24} In all experiments, erythrocytes were used immediately after isolation. Photohemolysis assays were performed by incubation in the dark the erythrocyte suspensions ($\sim 10^7$ red blood cells mL^{-1} , 2 mL in Pyrex tubes of $20 \times 50 \text{ mm}$) in PBS with porphyrins (1–5 μM) for 30 min at room temperature. Photosensitizers were added from a 0.5 mM stock solution in DMF. After incubation, the red blood cell suspension (2 mL) was exposed for different time periods to visible light. The light source used was a Novamat 130 AF slide projector equipped with a 150 W lamp. The light was filtered through a 2.5 cm glass cuvette filled with water to absorb heat. A wavelength range between 350–800 nm was selected by optical filters. The light fluence rate at the treatment site was 90 mW cm^{-2} (Radiometer Laser Mate-Q, Coherent). Photosensitized hemolysis of erythrocytes was carried out at room temperature. After irradiation, the samples were kept 24 h at room temperature in dark. After this time period the tubes were centrifuged and 100 μL of the supernatants were diluted in 2 mL of distilled water. The hemoglobin content was determined by measuring the absorbance at 413 nm. For studies in the absence of oxygen, the samples were deoxygenated by bubbling the samples with water-saturated argon for 15 min and then the solid-top caps were immediately sealed. Results are expressed as percentage of hemolysis taking 100% as the absorbance obtained from a sample lysed in distilled water.²² Control experiments were carried out without illumination in the absence and in the presence of

sensitizer as well as by irradiating the red blood cells without sensitizer. Each experiment was repeated at least three times.

Changes in cell morphology were analyzed under a microscope (Axiophot, Zeiss, Germany) using a color camera (AxioCam HRc, Zeiss, Germany) and processed with a AxioVision release 4.3 software.

Results and discussion

Absorption and fluorescence spectroscopic studies

The absorption spectra of porphyrins in DMF are shown in Fig. 1A. These sensitizers show the typical Soret and Q-bands, characteristic of a free-base H₂P and the corresponding metalloporphyrins.^{33,34} The Soret band absorption maximum of the porphyrins is summarized in Table 1. The spectra were also taken in benzene, methanol, BHDC reverse micellar system and PBS. In organic solvents, sharp absorption bands were obtained for H₂P, ZnP and CuP indicating that these porphyrins are mainly not aggregated in these media. The absorption bands showed a slight blue shift (~4 nm) upon solubilization in methanol with respect to a non-hydrogen bond donor, DMF. However, a low intensity and broadening of Soret band is observed in aqueous saline solution indicating that aggregation occurs as it is typical for many porphyrin derivatives.^{35,36} On the other hand, in these media the complex with Pd showed a broadening of the Soret band (Fig. 1A), indicating that PdP is not completely dissolved as monomer. The Soret absorption band of PdP in DMF obeyed the Beer–Lambert's law at concentrations of <0.2 μM (Fig. 1A, inset). Thus, aggregation occurs in DMF above certain PdP concentration.²⁶ From the data on the deviation from Beer–Lambert's law, an association constant for the dimerization of PdP of $6.5 \times 10^6 \text{ M}^{-1}$ was calculated in DMF.

The steady-state fluorescence emission spectra of these porphyrins were analyzed in DMF. As previously found for porphyrin derivatives forming complexes with Cu(II), no fluorescence bands were observed for CuP. In previous studies, a very low emission intensity was observed from complexes of porphyrins with Pd(II) with $\Phi_F \sim 10^{-4}$.^{14,16} However, in the present case the emission of PdP was negligible probably because its aggregation in this medium. The emission spectra of H₂P and ZnP are shown in Fig. 1B. The two bands are characteristic for free-base porphyrin ($\lambda_{\text{max}} = 651$ and 717 nm) and Zn(II) complex ($\lambda_{\text{max}} = 600$ and 658 nm). These bands have been assigned to Q(0–0) and Q(0–1) transitions.³⁴ The Stokes shifts were 4 and 6 nm for H₂P and ZnP, respectively. A small Stokes shift is expected for tetraphenylpor-

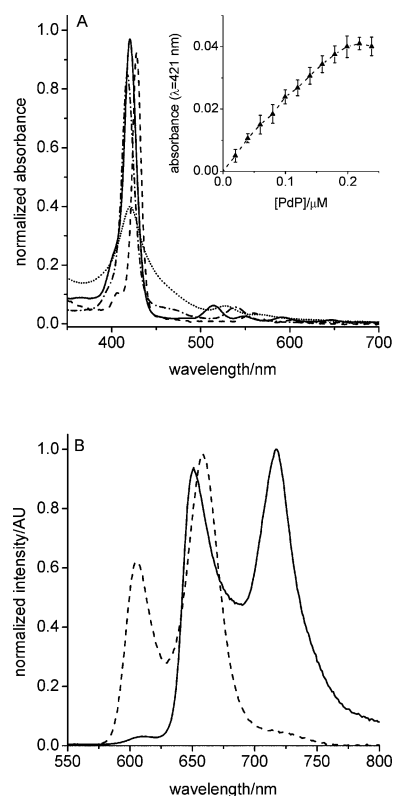


Fig. 1 (A) Absorption spectra of H₂P (solid line), ZnP (dashed line), PdP (dotted line) and CuP (dashed–dotted line), inset: variation of absorbance at 421 nm with PdP concentration; (B) fluorescence emission spectra of H₂P (solid line, $\lambda_{\text{exc}} = 515$ nm) and ZnP (dashed line, $\lambda_{\text{exc}} = 560$ nm) in DMF.

phyrin derivatives indicating that the spectroscopic energy is nearly identical to the relaxed energy of the singlet state.¹⁰ The values of Φ_F of the porphyrins were calculated by steady state comparative method using TPP as a reference (Table 1). Absorbances of sample and reference were matched at the respective excitation wavelength and the areas of the emission spectra were integrated in the range 575–850 nm. These results are in agreement with those previously reported for *meso*-substituted porphyrins in different media, such as TMP ($\Phi_F = 0.14$) and ZnTMP ($\Phi_F = 0.049$) in tetrahydrofuran.¹³ These Φ_F are suitable values for quantification and detection of the sensitizer in biological media. Moreover, a very low emission of fluorescence was found in PBS evidencing that these porphyrins are poorly soluble as monomer in this medium. The values calculated were $\Phi_F = 0.011 \pm 0.002$ for H₂P and

Table 1 Photophysical properties of porphyrins in DMF

	H ₂ P	ZnP	PdP	CuP
$\lambda_{\text{max}}^{\text{Soret}}/\text{nm}$	422	429	421	418
$\log \epsilon^{\text{Soret}}/\text{M}^{-1} \text{ cm}^{-1}$	5.17	5.13	4.92	5.10
$\lambda_{\text{max}}^{\text{Emission}}/\text{nm}$	651	605	—	—
E_s/eV	1.90 ± 0.02	2.04 ± 0.04	—	—
Φ_F	0.10 ± 0.01	0.067 ± 0.006	—	—
τ_s/ns	11.4 ± 0.1	2.60 ± 0.02	—	—
$\lambda_{\text{max}}^{\text{T}}/\text{nm}$	450	480	470	—
$\tau_T/\mu\text{s}$	176 ± 18	192 ± 20	44 ± 5	—
Φ_Δ	0.69 ± 0.05	0.59 ± 0.04	0.28 ± 0.03	—
$k_q^{\text{O}_2}/\text{M}^{-1} \text{ s}^{-1}$	$(12.0 \pm 0.7) \times 10^8$	$(9.5 \pm 0.5) \times 10^8$	$(8.8 \pm 0.4) \times 10^8$	—

$(6.3 \pm 0.6) \times 10^{-3}$ for ZnP in PBS. These lower values of Φ_F are due to an incomplete monomerization of porphyrins in the aqueous saline solution, since only monomer species fluoresce. Taking into account the porphyrin energy of the 0–0 electronic transitions the energy levels of the singlet excited state were calculated (Table 1) from the intersection of the normalized absorption and fluorescence spectra.

The lifetimes of the singlet excited state (τ_s , Table 1) of H₂P and ZnP are in agreement with information given in the literature ($\tau_s = 10.1$ for TPP and 2.7 for ZnTPP).^{37,38} The lifetime of ZnP excited singlet state is shorter than for H₂P and is significantly affected by the presence of a transition metal atom.

Triplet state and singlet oxygen production

Nanosecond laser flash photolysis allowed the observation of transient absorption of H₂P, ZnP and PdP in the range of 300–800 nm. The maximum absorption in the blue spectral region lies in the range of 440–500 nm for all the complexes. Representative results for ZnP are shown in Fig. 2. The triplet states of these compounds are efficiently quenched by oxygen (Table 1). The rate constant for oxygen quenching $k_q^{O_2} > 10^9 \text{ M}^{-1} \text{ s}^{-1}$ is controlled by the diffusion of oxygen.¹¹ In contrast, no transient absorption in the 300–800 nm region is observed for the CuP complex in DMF.

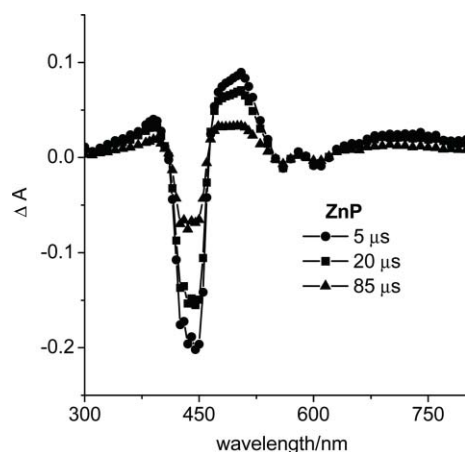


Fig. 2 Differential absorption spectra of ZnP after laser pulse excitation ($\lambda_{\text{exc}} = 532 \text{ nm}$) 5, 20 and 85 μs in oxygen free DMF.

The $O_2(^1\Delta_g)$ emission was measured at 1270 nm after laser excitation of the porphyrin solution. In the presence of air, the emission signal of $O_2(^1\Delta_g)$ formed in DMF showed a first-order exponential decay. The initial $O_2(^1\Delta_g)$ emission intensities (I_0) were calculated from extrapolation to zero time (determined by the laser shot). These initial signal intensities were plotted vs. laser total energy (between 0.1–1.0 mJ, Fig. 3). The quantum yield of $O_2(^1\Delta_g)$ production (Φ_Δ) was calculated from the slopes of the plots for the porphyrins compared to the corresponding slope obtained for the reference (TPP). The results for Φ_Δ (Table 1) follow the order H₂P \sim ZnP $>$ PdP, while formation of $O_2(^1\Delta_g)$ was not detected when CuP was used as photosensitizer. The value of Φ_Δ for H₂P is similar to those already reported for analogous porphyrin derivatives, such as TMP ($\Phi_\Delta = 0.65$).¹³

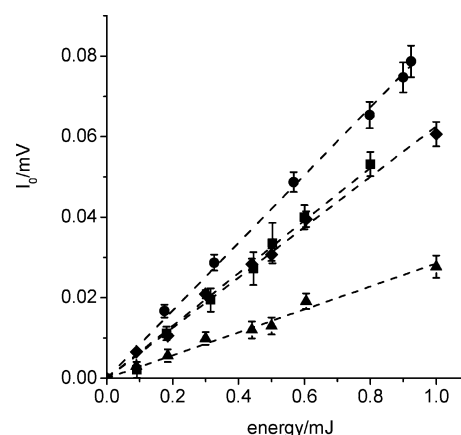


Fig. 3 Initial $O_2(^1\Delta_g)$ phosphorescence emission intensities (I_0 , $\lambda_{\text{em}} = 1270 \text{ nm}$) as a function of laser energies (E) of H₂P (●), ZnP (■), PdP (▲) and TPP (◆) in DMF.

Photosensitized decomposition of substrates in homogeneous medium

Photooxidation of 9,10-dimethylanthracene (DMA) sensitized by porphyrins was studied in DMF under aerobic condition (Fig. 4A). From first-order kinetic plots of the DMA absorption at 378 nm with time the values of the observed rate constant (k_{obs}) were calculated (Table 2). Free-base porphyrin and its complex with Zn(II) photodecompose DMA with similar rates. Under these conditions, a lower value of k_{obs} for DMA was obtained for the reaction sensitized by PdP. This result is expected since in DMF the cationic sensitizer is partially aggregated. The aggregates present an efficient non-radiative energy relaxation pathway, diminishing the triplet-state population and the $O_2(^1\Delta_g)$ quantum yield. Reaction of DMA sensitized by CuP was not detected.

Taking into account that DMA quenches $O_2(^1\Delta_g)$ exclusively by chemical reaction, it is used as a method to evaluate the ability of the sensitizers to produce $O_2(^1\Delta_g)$ in solution.³⁹ The quantum yield of $O_2(^1\Delta_g)$ production (Φ_Δ) were calculated by comparing the slope for the porphyrin with that for the reference (TPP, $k_{\text{obs}} = (11.5 \pm 0.1) \times 10^{-4} \text{ s}^{-1}$ in DMF) from the plots shown in Fig. 4A. Very close values of Φ_Δ were obtained for these porphyrins (Table 1 and Table 2) using both direct determination of $O_2(^1\Delta_g)$ by its phosphorescence at $\sim 1270 \text{ nm}$ and by DMA photodecomposition.

The nucleotide GMP was used as a model substrate for the compounds of biological interest that would be targets of porphyrin photosensitization.^{40,41} Continuous irradiation of porphyrins at 420 nm in air-saturated DMF leads to GMP decomposition as evidenced by the formation of a broad absorption band above 300 nm (Fig. 5A). Since under aerobic conditions the decomposition of GMP occurs predominantly through a type II photoreaction process, it was used to compare the sensitizing abilities of porphyrins. It is not possible to calculate the decomposition rate constant of GMP from these absorption data because of the overlap of the spectra of GMP with its degradations products.⁴⁰ However, it can be observed in Fig. 5A that H₂P and ZnP sensitize the decomposition of GMP faster than PdP. These results are in agreement with those of $O_2(^1\Delta_g)$ production.

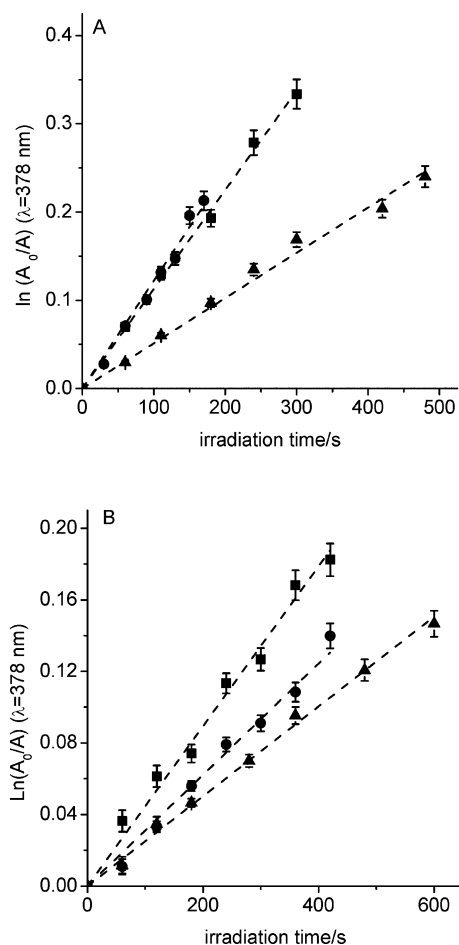


Fig. 4 First-order plots for the photooxidation of DMA (35 μM) photosensitized by H₂P (●), ZnP (■) and PdP (▲) in (A) DMF and (B) benzene/BHDC (0.1 M)/water ($W_0 = 10$) reverse micelles; $\lambda_{\text{irr}} = 515$ nm. Values represent the mean \pm standard deviation of three separate experiments.

Photodynamic activity in BHDC reverse micelles

The solubilization and interaction of these monocationic porphyrins were spectroscopically analyzed in benzene/BHDC (0.1 M)/water ($W_0 = 10$) reverse micelles. When the absorption spectra of porphyrins were studied at various BHDC concentrations, an increase in the intensity of the Soret band was observed as the surfactant concentration increased. This effect is attributed to the interaction between the porphyrin and the micelle. Plotting the left-hand side term of eqn (1) vs. $1/[\text{BHDC}]$, the value of the binding constant is calculated from the ratio of slope and the

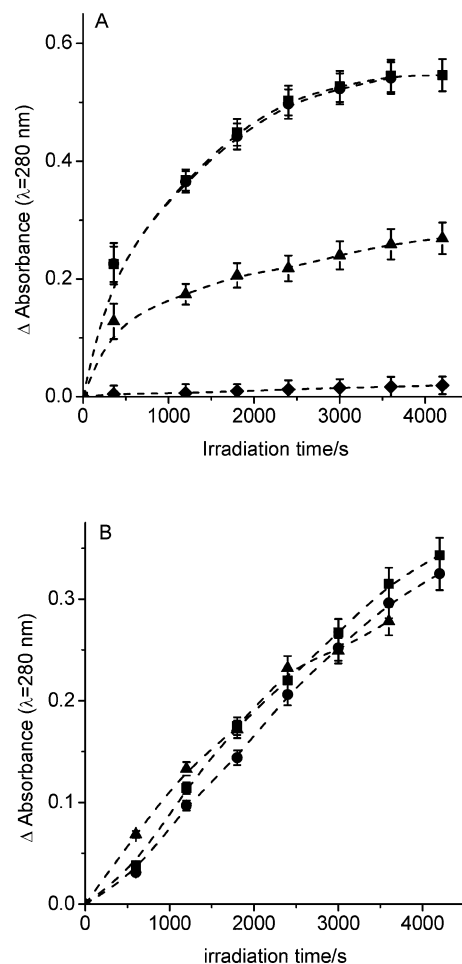


Fig. 5 Difference absorption spectra of GMP (100 μM) photooxidation sensitized by H₂P (●), ZnP (■), PdP (▲) and CuP (◆) at 280 nm in (A) DMF and (B) benzene/BHDC (0.1 M)/water ($W_0 = 10$) reverse micelles; $\lambda_{\text{irr}} = 420$ nm. Values represent the mean \pm standard deviation of three separate experiments.

intercept. Representative results are shown in Fig. 6 for H₂P. The large values of K_b for the free-base and metalloporphyrins (Table 2) indicate that in all cases the porphyrin is strongly associated with the micellar interface.

Moreover, the *n*-octanol/water partition coefficients of porphyrins (P) were evaluated at 25 °C ($P = [\text{porphyrin}]_0/[\text{porphyrin}]_w$). This parameter is used to evaluate the interaction of photosensitizers with biological systems. It is known that the *n*-octanol/water system mimics rather accurately the water/membrane interface. Thus, $\log P$ has been extensively utilized to predict the relative

Table 2 Porphyrin properties and kinetic parameters for the photooxidation of DMA

	H ₂ P	ZnP	PdP	CuP
$\log P$	0.97 ± 0.05	2.67 ± 0.09	0.93 ± 0.05	1.07 ± 0.08
K_b/M^{-1a}	4094 ± 300	1221 ± 100	1641 ± 150	812 ± 70
k_{obs}/s^{-1a}	$(12.2 \pm 0.06) \times 10^{-4}$	$(11.3 \pm 0.05) \times 10^{-4}$	$(5.1 \pm 0.2) \times 10^{-4}$	—
k_{obs}/s^{-1b}	$(3.1 \pm 0.1) \times 10^{-4}$	$(4.5 \pm 0.2) \times 10^{-4}$	$(2.5 \pm 0.1) \times 10^{-4}$	—
$\Phi_{\Delta}^{a,c}$	0.66 ± 0.05	0.58 ± 0.04	0.26 ± 0.03	—

^a DMF. ^b Benzene/BHDC (0.1 M)/H₂O ($W_0 = 10$). ^c Using TPP as reference.

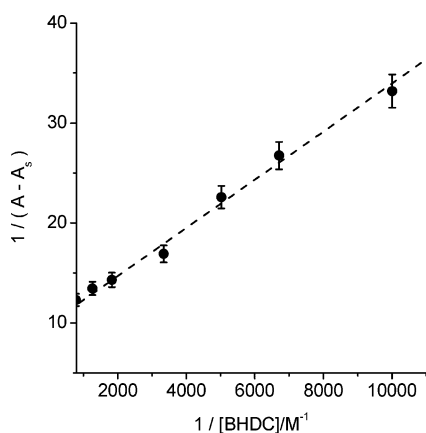


Fig. 6 Variation of $1/(A - A_{Bz})$ as a function of $1/[BHDC]$ for H_2P in benzene/BHDC (0.1 M)/water ($W_0 = 10$) reverse micelles. Dashed line: linear regression fit by eqn (1), $\lambda_{max} = 423$ nm.

tendency of compounds to interact with biological membranes.⁴² The lipophilic character is larger for ZnP (Table 2) than for free-base H_2P , whereas the complexation with Pd(II) and Cu(II) produces only small changes in the lipophilic character of the macrocycle. Photosensitizers with these log P values have shown a high intracellular accumulation, mainly determined by passive diffusion through the membrane.⁴³

Irradiation of the BHDC micelles containing DMA under aerobic conditions was performed in the presence of porphyrin. Because DMA is a non-polar compound, it should be mainly solubilized in the organic phase (benzene) of the micellar system.¹³ In this microenvironment, the substrate reacts with the $O_2(^1\Delta_g)$ photosensitized by porphyrin. From the plots in Fig. 4B, the values of the observed rate constant (k_{obs}) were calculated for DMA in micelles (Table 2). In contrast to the results in DMF, the complex with Zn(II) is the better photosensitizer to decompose DMA in micelles. Although the PdP sensitized DMA oxidation is slower than that sensitized by ZnP, the value of k_{obs} in the presence of PdP is quite similar to that of H_2P in micelles.

Under these conditions, photodecomposition of GMP follows the tendency showed in Fig. 5B. A similar behavior of H_2P , ZnP and PdP was found for the sensitized photooxidation of GMP in micelles. Even in this medium the complex with Cu(II) does not produce significant decomposition of GMP. These results confirm those obtained with DMA, indicating a higher photodynamic activity of PdP in the microheterogeneous medium. This effect can be due to a better solubilization of PdP(II) porphyrin as monomer in the microenvironment where the sensitizer is localized in the BHDC micelles. These results indicate that $O_2(^1\Delta_g)$ production is highly dependent on the medium where the sensitizer is localized and considerably decreases when the sensitizer is aggregated.

Photohemolysis of human erythrocytes cells

Photohemolysis of human erythrocyte cells was used to evaluate *in vitro* the photodynamic activity of porphyrins in a biomimetic membrane model.¹⁹⁻²⁴ Spectroscopic measurements of hemoglobin are much easier and faster to carry out than cell staining and counting. This is an advantage of using red blood cells for this type of investigation.²⁵

Cell toxicity induced by the photosensitizers was first analyzed in the dark. The erythrocytes cell suspensions were treated with 1–5 μM of sensitizers for 30 min at room temperature. Under these experimental conditions, H_2P , ZnP and CuP produced no significant hemolysis. Light alone at the highest fluence rate used, did not induce photohemolysis. Therefore, the hemolysis obtained after irradiation of the erythrocytes cells treated with the porphyrins is due to the photosensitization effect of the agent produced by visible light. In contrast, PdP is toxic in the dark producing 36% and 63% of cellular hemolysis when the erythrocytes are treated with 1 and 5 μM of sensitizer, respectively.

The corresponding cellular photolytic activities for each photosensitizer are shown in Fig. 7. The hemolysis of red blood cells irradiated with visible light depended on the light exposure. The photohemolytic effect is higher with H_2P than with ZnP, when cells are treated with 1 μM sensitizer (Fig. 7A). Even though PdP produces hemolysis in the dark, the activity increases $\sim 20\%$ after 30 min of irradiation. Under these conditions, CuP shows

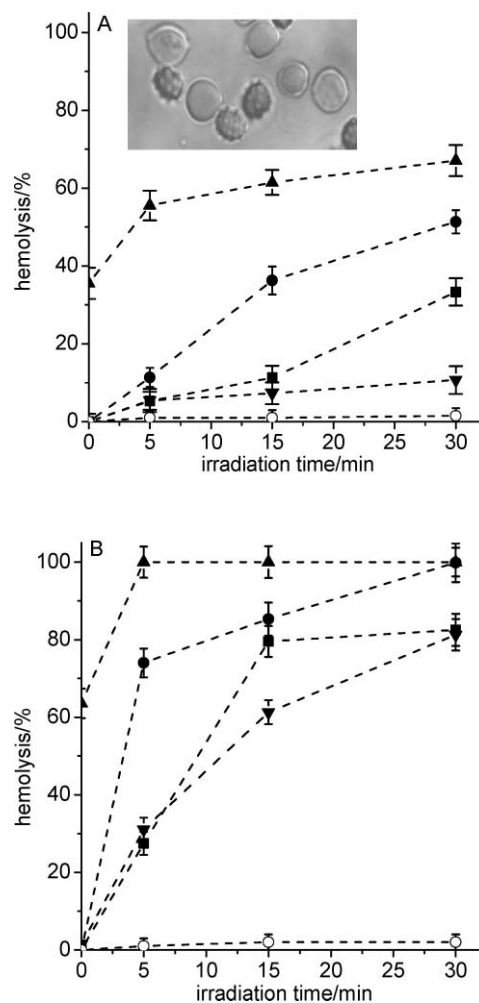


Fig. 7 Photohemolysis of human red blood cells treated with (A) 1 μM and (B) 5 μM of H_2P (●), ZnP (■), PdP (▲) and CuP (▼) for 30 min in dark and irradiated with visible light for different irradiation times. Control culture untreated with sensitizer and irradiated (○). Values represent mean \pm standard deviation of three separate experiments. The inset in (A) is a photograph showing the morphology of erythrocytes treated with 1 μM H_2P and irradiated for 15 min (100 \times microscope objective).

a low photohemolytic efficiency, probably due to its very small formation of $O_2(^1\Delta_g)$. These observations are consistent with the reported lack of type II activity for a complex with Cu(II), which is presumed to undergo a type I photodynamic response.⁴⁴ Removal of Cu(II) from the macrocycle increases the possibility of a type II mechanism, which is the case of H_2P . These results are in agreement with those found in solution, in which H_2P and ZnP produce efficiently $O_2(^1\Delta_g)$. This behavior is not always expected in cellular media, where the biological microenvironment of the sensitizer can induce significant changes in the photophysics of the porphyrin with respect to those observed in solution.⁴⁵

The morphology of erythrocytes was observed by microscopy after incubation with 1 μM of sensitizer and irradiated for 15 min. Representative results for H_2P are shown in Fig. 7A (inset). The microscopic observations show that the red cells changed their normal biconcave discoid shape and present a cell surface characterized by spikes and blebs. This effect was present in all studied samples with partial photohemolysis. Similar deformation of membrane has been previously found in oxidative damage of human erythrocytes.⁴⁶

When the cells are incubated with 5 μM sensitizer (Fig. 7B), the hemolysis of erythrocytes considerably increases, reaching a value of 100% for H_2P after 30 min of irradiation. The photodynamic activity follows the tendency showed above for 1 μM , *i.e.*, $H_2P > ZnP$. Although, PdP produces 100% of hemolysis after 5 min of irradiation, it is considerable hemolytic in dark. The main difference is found with CuP, which is almost as effective as ZnP using this high concentration.

To evaluate the influence of oxygen atmosphere, the photohemolysis of erythrocytes cells was analyzed under anoxic conditions. Irradiation of the cellular suspension treated with 5 μM of sensitizer was performed under argon atmosphere. After 15 min of light, the hemolysis was 34, 20 and 22% for H_2P , ZnP and CuP, respectively. In all cases the hemolytic effect was oxygen dependent. Cell hemolysis even occurs using these porphyrins as sensitizer under a low oxygen concentration. Moreover, rather large amount of damage are still produced when experiments are performed under argon atmosphere, which are not expected for a singlet oxygen-driven chemistry. Therefore, alternative type I photoreaction pathways, which involve a direct interaction between the excited photosensitizer and the substrate, could be occurring under reduced oxygen atmosphere. However, these results can not be used to establish the predominant mechanism of photoreaction produced by the photosensitizers used in this study.⁴⁷

Conclusions

This study provides information on the photophysical and photodynamic activity of amphiphilic monocationic porphyrin derivatives in different systems. Porphyrins and metallo porphyrins readily aggregate in solution even at low concentration. In our case, this is the main problem that affects the behavior of PdP as a possible photosensitizer, since the formation of aggregates leads to a decrease in the lifetime of the triplet excited state.¹¹ This is not the case of H_2P and ZnP, which are mainly solubilized as monomers in DMF. The value of τ_T for PdP is four times lower than that of the free-base porphyrin under identical conditions. This shorter triplet lifetime could be due to aggregation. However, the decrease

of the triplet lifetime of the Pd complex may also be due to heavy atom effect. The effect of aggregation is evidenced in the relatively low value of Φ_Δ found for PdP ($\Phi_\Delta = 0.28$) in comparison with literature data for Pd(II) tetraphenylporphyrin ($\Phi_\Delta \sim 0.78-0.88$).³² On the other hand, CuP is a radiationless metalloporphyrin and its triplet state was not observed in solution.

In BHDC, all of these porphyrins strongly interact with the micelles. In this medium, it could be assumed that amphiphilic porphyrins localize at the interface with the cationic group in the polar part of the reverse micelle and the porphyrin skeleton near the apolar phase. In particular, solubilization of PdP in reverse micelles is apparently accompanied by disruption of the non-covalent aggregates. Thus, in this microheterogenic medium PdP has a similar photodynamic effect as found for H_2P and ZnP.

Human erythrocytes represent a convenient model for studies of fundamental principles of PDT. Therefore, these cells were used to evaluate the capacity of these sensitizers to produce membrane photodamage. H_2P was the most effective photosensitizer to induce hemolysis of red blood cells. After treatment with 5 μM sensitizer, the values of the light exposure level required to produce 50% of cell hemolysis were 18 ± 2 , 48 ± 5 and 60 ± 5 J cm^{-2} for H_2P , ZnP and CuP, respectively. A larger difference with the sensitizer concentration was found for CuP. Cells treated with 1 μM CuP produce <10% of hemolysis, whereas the hemolytic activity increases up to $\sim 70\%$ in the presence of 5 μM after 30 min of irradiation with visible light. In aerobic conditions it is accepted that $O_2(^1\Delta_g)$ is probably the main species responsible for photodamage using sensitizers with high Φ_Δ .⁴⁸ In the present study, it was observed that the photohemolytic process considerably decreases under anoxic conditions. Furthermore, even if an excited photosensitizer reacts with a given substrate by type I photoprocess, the final result is also the oxidation of essential biomolecules.⁴⁹ The main novel result from this studies is that the formation of metallo complexes with Zn(II) and Pd(II) is not accompanied by a significant increase in the photodynamic activity neither in solution nor in erythrocyte cells.

Acknowledgements

The authors thank Consejo Nacional de Investigaciones Científicas y Técnicas (CONICET) of Argentina, SECYT Universidad Nacional de Río Cuarto and Agencia Nacional de Promoción Científica y Tecnológica (ANPCYT) of Argentina for financial support. M. G. A., S. G. B. and E. N. D. are Scientific Members of CONICET. M. E. M. thanks CONICET for a doctoral fellowship.

References

- 1 A. P. Castano, T. N. Demidova and M. R. Hamblin, Mechanisms in photodynamic therapy: part one - photosensitizers, photochemistry and cellular localization, *Photodiagn. Photodynam. Therapy*, 2004, **1**, 279–293.
- 2 A. Mitra and G. I. Stables, Topical photodynamic therapy for non-cancerous skin conditions, *Photodiagn. Photodynam. Therapy*, 2006, **3**, 116–127.
- 3 E. N. Durantini, Photodynamic inactivation of bacteria, *Curr. Bioactive Compd.*, 2006, **2**, 127–142.
- 4 G. Jori, Photodynamic therapy of microbial infections: state of the art and perspectives, *J. Environ. Pathol. Toxicol. Oncol.*, 2006, **25**, 505–519.
- 5 M. Ochsner, Photophysical and photobiological processes in photodynamic therapy of tumours, *J. Photochem. Photobiol., B*, 1997, **39**, 1–18.

- 6 M. C. DeRosa and R. J. Crutchley, Photosensitized singlet oxygen and its applications, *Coord. Chem. Rev.*, 2002, **233–234**, 351–371.
- 7 K. Lang, J. Mosinger and D. M. Wagnerová, Photophysical properties of porphyrinoid sensitizers non-covalently bound to host molecules; models for photodynamic therapy, *Coord. Chem. Rev.*, 2004, **248**, 321–350.
- 8 M. R. Detty, S. T. Gibson and S. J. Wagner, Current clinical photosensitizers for use in photodynamic therapy, *J. Med. Chem.*, 2004, **47**, 3897–3915.
- 9 H. Ali and J. E. van Lier, Metal complexes as photo- and radiosensitizers, *Chem. Rev.*, 1999, **99**, 2379–2450.
- 10 M. Pineiro, A. L. Carvalho, M. M. Pereira, A. M. d'A. Rocha Gonsalves, L. G. Arnaut and S. J. Formosinho, Photoacoustic measurements of porphyrin triplet-state quantum yields and singlet-oxygen efficiencies, *Chem.–Eur. J.*, 1998, **4**, 2299–2307.
- 11 P. Kubát and J. Mosinger, Photophysical properties of metal complexes of *meso*-tetrakis(4-sulfonatophenyl)porphyrin, *J. Photochem. Photobiol., A*, 1996, **96**, 93–97.
- 12 G. M. Garbo, V. H. Fingar, T. J. Wieman, E. B. Noakes III, P. S. Haydon, P. B. Cerrito, D. H. Kessel and A. R. Morgan, *In vivo* and *in vitro* photodynamic studies with benzochlorin iminium salts delivered by a lipid emulsion, *Photochem. Photobiol.*, 1998, **68**, 561–568.
- 13 M. E. Milanesio, M. G. Alvarez, E. I. Yslas, C. D. Borsarelli, J. J. Silber, V. Rivarola and E. N. Durantini, Photodynamic studies of metallo 5,10,15,20-tetrakis(4-methoxyphenyl) porphyrin: photochemical characterization and biological consequences in a human carcinoma cell line, *Photochem. Photobiol.*, 2001, **74**, 14–21.
- 14 J. E. Rogers, K. A. Nguay, D. C. Hufnagle, D. G. MaLean, W. Su, K. M. Gossett, A. R. Burke, S. A. Vinogradov, R. Pachter and P. A. Fleitz, Observation and interpretation of annulated porphyrins: studies on the photophysical properties of *meso*-tetraphenylmetalloporphyrins, *J. Phys. Chem. A*, 2003, **107**, 11331–11339.
- 15 J. J. Silber, A. Biasutti, E. Abuin and E. Lissi, Interactions of small molecules with reverse micelles, *Adv. Colloid Interface Sci.*, 1999, **82**, 189–252.
- 16 I. Scalise and E. N. Durantini, Photodynamic effect of metallo 5-(4-carboxyphenyl)-10,15,20-tris(4-methylphenyl) porphyrins in biomimetic media, *J. Photochem. Photobiol., A*, 2004, **162**, 105–113.
- 17 S. M. S. Chauhan, P. P. Mohapatra, B. Kalra, T. S. Kohli and S. Satapathy, Biomimetic oxidation of indole-3-acetic acid and related substrates with hydrogen peroxide catalysed by 5,10,15,20-tetrakis(2',6'-dichloro-3'-sulfonatophenyl)porphyrinatoiron(III) hydrate in aqueous solution and AOT reverse micelles, *J. Mol. Catal., A*, 1996, **113**, 239–247.
- 18 S. M. S. Chauhan and B. B. Sahoo, Biomimetic oxidation of ibuprofen with hydrogen peroxide catalysed by Horseradish peroxidase (HRP) and 5,10,15,20-tetrakis(2',6'-dichloro-3'-sulfonatophenyl)porphyrinatoiron(III) and manganese(III) hydrates in AOT reverse micelles, *Bioorg. Med. Chem.*, 1999, **72**, 629–2634.
- 19 A. Juarranz, A. Villanueva, V. Diaz, L. Rodríguez-Borlado, C. Trigueros and M. Cañete, Induced photolysis of rabbit red blood cells by several photosensitizers, *Anti-Cancer Drugs*, 1993, **4**, 501–504.
- 20 I. Rosenthal, V. Y. Shafirovich, N. E. Geacintov, E. Ben-Hur and B. Horowitz, The photochemical properties of fluoroaluminum phthalocyanine, *Photochem. Photobiol.*, 1994, **60**, 215–220.
- 21 M. Khalili and L. I. Grossweiner, Sensitization of photohemolysis by benzoporphyrin derivative monoacid ring A and porphyrins, *J. Photochem. Photobiol., B*, 1997, **37**, 236–244.
- 22 M. Hoebeke, H. J. Schuitmaker, L. E. Jannink, T. M. A. R. Dubbelman, A. Jakobs and A. Van de Vorst, Electron spin resonance evidence of the generation of superoxide anion, hydroxyl radical and singlet oxygen during the photohemolysis of human erythrocytes with bacteriochlorin a, *Photochem. Photobiol.*, 1997, **66**, 502–508.
- 23 A. Marozienė, R. Kliukienė, J. Šarlauskas and N. Čenas, Inhibition of phthalocyanine-sensitized photohemolysis of human erythrocytes by polyphenolic antioxidants: description of quantitative structure-activity relationships, *Cancer Lett.*, 2002, **157**, 39–44.
- 24 I. B. Zavodnik, L. B. Zavodnik and M. J. Bryszewska, The mechanism of Zn-phthalocyanine photosensitized lysis of human erythrocytes, *J. Photochem. Photobiol., B*, 2002, **67**, 1–10.
- 25 L. Kaestner, A. Juzeniene and J. Moan, Erythrocytes - the 'house elves' of photodynamic therapy, *Photochem. Photobiol. Sci.*, 2004, **3**, 981–989.
- 26 M. E. Milanesio, M. G. Alvarez, J. J. Silber, V. Rivarola and E. N. Durantini, Photodynamic activity of monocationic and non-charged methoxyphenyl porphyrin derivatives in homogeneous and biological medium, *Photochem. Photobiol. Sci.*, 2003, **2**, 926–933.
- 27 M. G. Alvarez, F. Principe, M. E. Milanesio and V. Rivarola, Photodynamic damage induced by a monocationic porphyrin derivative in a human carcinoma cell line, *Int. J. Biochem. Cell Biol.*, 2005, **37**, 2504–2512.
- 28 M. G. Alvarez, N. B. Rumie Vittar, F. Principe, J. R. Bergesse, M. C. Romanini, S. Romanini, M. Bertuzzi and V. Rivarola, Pharmacokinetic and phototherapeutic studies of monocationic methoxyphenylporphyrin derivative, *Photodiagn. Photodynam. Therapy*, 2004, **1**, 335–344.
- 29 G. Valduga, S. Nonell, E. Reddi, G. Jori and S. E. Braslavsky, The production of singlet molecular oxygen by zinc(II) phthalocyanine in ethanol and in unilamellar vesicles. Chemical quenching and phosphorescence studies, *Photochem. Photobiol.*, 1988, **48**, 1–5.
- 30 J. D. Spikes, Quantum yields and kinetics of the photobleaching of hematoporphyrin, photofrin II, tetra(4-sulfonatophenyl)-porphine and uroporphyrin, *Photochem. Photobiol.*, 1992, **55**, 792–808.
- 31 H. A. Montejano, M. Gervaldo and S. G. Bertolotti, The excited-states quenching of resazurin and resorufin by *p*-benzoquinones in polar solvents, *Dyes Pigm.*, 2005, **64**, 117–124.
- 32 R. W. Redmond and J. N. Gamlin, A compilation of singlet yields from biologically relevant molecules, *Photochem. Photobiol.*, 1999, **70**, 391–475.
- 33 R. Bonnett, S. Ioannou, A. G. James, C. W. Pitt and M. M. Z. Soe, Synthesis and film-forming properties of metal complexes of octadecyl ethers of 5,10,15,20-tetrakis(4-hydroxyphenyl) porphyrin, *J. Mater. Chem.*, 1993, **3**, 793–799.
- 34 D. J. Quimby and F. R. Longo, Luminescence studies on several tetraarylporphyrins and their zinc derivatives, *J. Am. Chem. Soc.*, 1975, **97**, 5111–5117.
- 35 D. L. Akins, H.-R. Zhu and C. Guo, Aggregation of tetraaryl-substituted porphyrins in homogeneous solution, *J. Phys. Chem.*, 1996, **100**, 5420–5425.
- 36 G. Csík, E. Balog, I. Voszka, F. Tölgyesi, D. Oulmi, Ph. Maillard and M. Momenteau, Glycosylated derivatives of tetraphenyl porphyrin: photophysical characterization, self-aggregation and membrane binding, *J. Photochem. Photobiol., B*, 1998, **44**, 216–224.
- 37 J. W. Owens, R. Smith, R. Robinson and M. Robins, Photophysical properties of porphyrins, phthalocyanines and benzochlorins, *Inorg. Chim. Acta*, 1998, **279**, 226–231.
- 38 S. L. Murov, I. Carmichael and G. L. Hug, *Handbook of Photochemistry, Revised and Expanded*, M. Dekker, New York, 2nd edn, 1993.
- 39 A. Gomes, E. Fernandes and J. L. F. C. Lima, Fluorescence probes used for detection of reactive oxygen species, *J. Biochem. Biophys. Methods*, 2005, **65**, 45–80.
- 40 P. Kubát, K. Lang, P. Anzenbacher Jr., K. Jursíková, V. Král and B. Ehrenberg, Interaction of novel cationic *meso*-tetraphenylporphyrins in the ground and excited states with DNA and nucleotides, *J. Chem. Soc., Perkin Trans. 1*, 2000, 933–941.
- 41 K. Hirakawa, S. Kawanishi, T. Hirano and H. Segawa, Guanine-specific DNA oxidation photosensitized by the tetraphenylporphyrin phosphorus(V) complex via singlet oxygen generation and electron transfer, *J. Photochem. Photobiol., B*, 2007, **87**, 209–217.
- 42 F. M. Engelmann, S. V. O. Rocha, H. E. Toma, K. Araki and M. S. Baptista, Determination of *n*-octanol/water partition and membrane binding of cationic porphyrins, *Int. J. Pharm.*, 2007, **329**, 12–18.
- 43 J. C. Stockert, A. Juarranz, A. Villanueva, S. Nonell, R. W. Horobin, A. T. Soltermann, V. Rivarola, L. L. Colombo, J. Espada and M. Cañete, Photodynamic therapy: selective uptake of photosensitizing drugs into tumor cells, *Curr. Top. Pharmacol.*, 2004, **8**, 185–217.
- 44 J. A. Hampton, D. Skalkos, P. M. Taylor and S. H. Selman, Iminium salt of copper benzochlorin (CDS1), a novel photosensitizer for photodynamic therapy: mechanism of cell killing, *Photochem. Photobiol.*, 1993, **58**, 100–105.
- 45 B. M. Aveline and R. W. Redmond, Can cellular phototoxicity be accurately predicted on the basis of sensitizer photophysics?, *Photochem. Photobiol.*, 1999, **69**, 306–316.

-
- 46 M. Suwalsky, P. Orellana, M. Avello and F. Villena, Protective effect of *Ugni molinae* Turcz against oxidative damage of human erythrocytes, *Food Chem. Toxicol.*, 2007, **45**, 130–135.
- 47 B. M. Aveline, R. M. Sattler and R. W. Redmond, Environmental effects on cellular photosensitization: correlation of phototoxicity mechanism with transient absorption spectroscopy measurements, *Photochem. Photobiol.*, 1998, **68**, 51–62.
- 48 G. Jori, L. Schindl, A. Schindl and L. Polo, Novel approaches towards a detailed control of the mechanism and efficiency of photosensitized process *in vivo*, *J. Photochem. Photobiol., A*, 1996, **102**, 101–107.
- 49 T. M. A. R. Dubbelman and J. Steveninck, Photodynamically induced damage to cellular functions and its relation to cell death, *J. Photochem. Photobiol., B*, 1990, **6**, 345–347.